



Lautenschlager, S. (2016). Digital reconstruction of soft-tissue structures in fossils. *Journal of Paleontology*, 22, 101-117.
<https://doi.org/10.1017/scs.2017.10>

Peer reviewed version

Link to published version (if available):
[10.1017/scs.2017.10](https://doi.org/10.1017/scs.2017.10)

[Link to publication record in Explore Bristol Research](#)
PDF-document

This is the author accepted manuscript (AAM). The final published version (version of record) is available online via Cambridge University Press at <https://www.cambridge.org/core/journals/the-paleontological-society-papers/article/digital-reconstruction-of-softtissue-structures-in-fossils/24675D2D2A93CC888ED92671FE1B34B9>. Please refer to any applicable terms of use of the publisher.

University of Bristol - Explore Bristol Research

General rights

This document is made available in accordance with publisher policies. Please cite only the published version using the reference above. Full terms of use are available:
<http://www.bristol.ac.uk/pure/about/ebr-terms>

DIGITAL RECONSTRUCTION OF SOFT-TISSUE STRUCTURES IN FOSSILS

Stephan Lautenschlager*

School of Earth Sciences, University of Bristol, Life Sciences Building, 24 Tyndall Avenue,
Bristol BS8 1TQ, UK

*Corresponding author: glzsl@bristol.ac.uk

ABSTRACT.—In the last two decades, advances in computational imaging techniques and digital visualization have created novel avenues for the study of fossil organisms. As a result, paleontology has undergone a shift from the study of fossilized bones, teeth, and other hard-tissues to using virtual computer models to study specimens in greater detail, restore incomplete specimens, and perform biomechanical analyses. The rapidly increasing application of these techniques further paved the way for the digital reconstruction of soft-tissue structures, which are rarely preserved in the fossil record. In this contribution, different types of digital soft-tissue reconstructions are introduced and reviewed. Examples include methodological approaches for the reconstruction of musculature, endocranial components (i.e., brain, inner ear, neurovascular structures), and other soft-tissues (e.g., whole-body and life reconstructions). Digital techniques provide versatile tools for the reconstruction of soft-tissues, but given the nature of fossil specimens some limitations and uncertainties remain. Nevertheless, digital reconstructions can provide new information, in particular if interpreted in a phylogenetically grounded framework. Combined with other digital analysis techniques, such as finite element analysis (FEA), multibody dynamics analysis (MDA) and computational fluid dynamics (CFD), soft-tissue reconstructions can be used to elucidate the paleobiology of extinct organisms and to test competing evolutionary hypotheses.

INTRODUCTION

Fossils form the only physical evidence of extinct life and our knowledge of past organisms and ecosystems almost entirely depends on their presence and preservation. The

28 vast majority of fossils consist of bones and teeth in vertebrates, biomineralized shells and
29 exoskeletons in invertebrates, trace fossils, and other diagenetically persistent structures (i.e.,
30 spores, pollen) (Schopf, 1975). In contrast, soft-tissues are only rarely preserved in the fossil
31 record. Although a few examples of exceptional preservation have allowed remarkably
32 detailed insights into the soft-tissue anatomy of extinct vertebrates (Sasso and Signore, 1998;
33 Trinajstić et al., 2007; Schweitzer, 2011), invertebrates (Butterfield, 2003; Sutton et al.,
34 2005), and plants (Gerrienne et al., 2006; Bernard et al., 2007), these cases generally form the
35 exception rather than the rule (Allison and Briggs, 1993; Wilby and Briggs, 1997). However,
36 detailed knowledge of soft-tissue structures is paramount to understanding the paleobiology
37 of extinct organisms (Witmer, 1995): 1) Soft-tissues are responsible for a multitude of
38 physiological functions, such as locomotion, breathing, or temperature regulation; 2) soft-
39 tissues can drastically change the appearance of an organism in comparison to its preserved
40 hard parts; 3) soft-tissue characters can provide important phylogenetic information; and 4)
41 soft-tissues control the development and shaping of hard-tissues. As paleontologists, we are
42 therefore challenged with the reconstruction of such anatomical components, which have not
43 been mineralized and preserved, in order to understand fossils as living, functioning
44 organisms.

45 As a consequence, soft-tissue reconstructions have a long history, in particular in
46 vertebrate paleontology. Traditionally, the presence and arrangement of soft-tissues has been
47 inferred on the basis of the preserved hard parts or in comparison with extant taxa, which
48 form a phylogenetic bracket or a functional analogue (Bryant and Russell, 1992; Witmer,
49 1995). In the past, such soft-tissue reconstructions have generally been performed in a
50 theoretical framework and in the form of two-dimensional drawings and schematics. This
51 includes, for example, the reconstruction of musculature in different vertebrates (Adams,
52 1918; Romer, 1923; Miner, 1925; Barghusen, 1973; Sumida, 1989) and some invertebrate

53 groups (Budd, 1998), pneumatic and pulmonary structures (Witmer, 1997; O’Connor, 2006),
54 and other soft-tissues (Frey et al., 2003).

55 In recent years, the advent of novel computational techniques has dramatically
56 changed the ways in which fossils can be studied and characterized (Cunningham et al.,
57 2014). First and foremost, computed tomography (CT) now allows new insights into fossils,
58 and the identification and visualization of internal structures (Sutton, 2008). Functional
59 analyses, such as finite element analysis (FEA), multibody dynamics analysis (MDA), or
60 computational fluid dynamics (CFD), based on digital models of fossils provide the means
61 for biomechanical studies and to quantify fossil function (Rayfield, 2007; Curtis, 2011;
62 Rahman et al., 2015). Digital techniques further provide powerful tools to restore the hard-
63 tissue morphology of fossils and to remove taphonomic and preservational artefacts
64 (Lautenschlager, 2012; Cunningham et al., 2014; Lautenschlager et al., 2014b). Similarly, the
65 same methods have been used to reconstruct various soft-tissues in fossils (Fig. 1). However,
66 as soft-tissue reconstructions rely greatly on the preserved hard-tissues, this approach has
67 largely been restricted to vertebrate fossils in the past, but could easily be applied (with some
68 limitations) to non-vertebrate fossils. This contribution provides an overview of existing
69 examples of soft-tissue reconstructions and reviews applied techniques and methods.

70

71

DEFINITIONS

72 The popularity of digital methods to visualize and analyze fossils three-dimensionally has led
73 to a variety of different terminologies – none of which, however, are clearly defined. As a
74 result, the term “digital reconstruction” is often used ambiguously. This term has been used to
75 describe the visualization of a physical specimen following its digitization; as such it is
76 synonymous with the meaning of “digital representation” of the specimen, and the latter term
77 is advocated here for this purpose. In contrast, digital reconstruction is used here in the

78 context of recreating and visualizing anatomical structures, which are not preserved and
79 directly observable. In addition, “digital restoration” is used as a further term to describe the
80 process of removing preservational artefacts to restore the original morphology of a specimen
81 as prior to fossilization.

82

83

MUSCULATURE

84 **Examples**

85 Muscles form an integral part of an animal's anatomy and play a fundamental role in
86 feeding, locomotion, and other physiological activities. Unsurprisingly, numerous studies
87 have focussed on the reconstruction of various parts of the musculature in fossils (e.g., Dilkes
88 et al., 2012 and references therein) and the same is true for digital, three-dimensional
89 reconstructions of musculoskeletal anatomy (Fig. 1A). The increased popularity of
90 biomechanical modelling techniques, such as FEA or MDA, have further created demand and
91 renewed interest in detailed and accurate muscle reconstructions to serve as input parameters
92 for computational analyses (Bright, 2014). Driven by biomechanical studies, digital
93 reconstructions have focussed mostly on the cranial jaw adductor musculature and the
94 locomotory muscle complex in vertebrates.

95 Digital reconstructions of the jaw adductor muscles have been created for different
96 vertebrate groups, including dinosaurs (Lautenschlager, 2013; Button et al., 2014; Cuff and
97 Rayfield, 2015), pliosaurs (Foffa et al., 2014), and marsupials and fossil placental mammals
98 (Wroe et al., 2013; Cherin et al., 2014; Sharp, 2014). However, variations exist as to how
99 detailed the different muscle groups were reconstructed and to what further purpose.

100 Similarly, reconstructions of postcranial muscles have been created to study dinosaurian
101 locomotory capabilities (Hutchinson et al., 2005; Persons and Currie, 2011b; Sellers et al.,
102 2013) and feeding behaviour (Snively et al., 2013).

103

104 **Methodological approach**

105 The identification of the muscle attachment sites forms the basis of all digital muscle
106 reconstructions, regardless of whether they are performed on the cranial skeleton, postcranial
107 elements, or in invertebrates (Lautenschlager, 2013) (Fig. 2A). Identification is performed
108 either on the actual specimen (if available) or the digital model; ideally both, as some
109 (osteological) correlates might only be visible on the physical specimen and vice versa.
110 Correlates attributable to muscle attachment are usually preserved in the form of distinct
111 surface features, such as bony ridges and projections, depressions, rugosities, and muscle
112 scars. Further features constraining not only the position but also the extent of the muscle
113 attachment may be consulted if present. In this, the digital approach is comparable to
114 traditional muscle reconstructions (e.g., Dilkes, 1999; Holliday, 2009).

115 Following the identification of the muscle attachment sites, the three-dimensional
116 muscle arrangement can be reconstructed. As the majority of muscles are suspended between
117 their origin and insertion, a point-to-point connection will allow a simplified visualization of
118 the muscle topology (Fig. 2B). In most instances, more than one muscle or muscle group
119 attaches to the skeletal element of interest (e.g., the mandible) and the creation of simplified
120 muscle connections will provide further constraints on the muscle arrangement. For example,
121 between three and 10 jaw adductor muscles occupy the cranial skeleton in vertebrates. The
122 different muscles will have to be accommodated within this bony housing without
123 intersection, imposing further “packing-constraints”. For the digital reconstruction, this can
124 mean that muscle attachments might have to be revisited in a recursive approach in order to
125 produce a compatible muscle arrangement for the simplified muscles represented by point-to-
126 point connections. However, the use of digital models usually permits rearranging these
127 simplified muscles without too much effort and testing different configurations. The number

128 of muscles to be reconstructed and hard-tissue constraints depend largely on the anatomical
129 region and taxonomic group, thereby offering more or less information on the placement and
130 muscle arrangement.

131 Depending on the type of subsequent analysis, the simplified muscle reconstruction
132 may already be sufficient. For the investigation of muscle strain (Lautenschlager, 2015) (Fig.
133 2C) or muscle moment arms (Chapman et al., 2010), simplified muscle reconstructions have
134 been used in the past. Similarly, studies involving multibody dynamics analysis rely largely
135 on the position and orientation of muscles (Hutchinson et al., 2005; Curtis et al., 2008;
136 Moazen et al., 2008; Bates and Falkingham, 2012) to calculate kinematic behavior. A similar
137 approach has been applied for finite element analysis, an engineering technique, which
138 calculates the magnitude and distribution of stress and strain in geometric objects in response
139 to loading regimes, such as muscle forces. In the past, these muscle forces have mostly been
140 applied to individual points (i.e., nodes) of the finite element (FE) models in the form of force
141 vectors (Rayfield, 2007; Dumont et al., 2009). Information on the location and direction of
142 these force vectors can be obtained from simplified muscle reconstructions. More recently,
143 further techniques have been proposed to model muscles wrapping around bone to replicate
144 actual muscle attachment in FE models (Grosse et al., 2007; Liu et al., 2012). However, this
145 approach requires data on the three-dimensional muscle morphology. Furthermore, to
146 calculate different muscle properties (volume, cross-section area, mass) and muscle forces, a
147 more detailed “fleshed-out” reconstruction is necessary.

148 Different approaches exist to create a full muscle reconstruction and these depend
149 largely on the type of models (surface-based vs tomographic) and the software used. For
150 tomographic datasets, special segmentation software, such as Avizo (VSG, Visualization
151 Science Group), Mimics (Materialise), or SPIERS (Sutton et al., 2012) can be used to
152 increase the diameter of the simplified muscle connections isometrically until connections of

153 the same muscle merge into another, or until other muscle groups or osteological/hard tissue
154 boundaries are encountered (Lautenschlager, 2013) (Fig. 2D). This is based on the
155 assumption that all muscles are increased by the same amount, but this can be adjusted if
156 further information is available giving precedence of one muscle over the other. For surface-
157 based data, it is possible to virtually sculpt muscles on top of digital skeletal elements, aided
158 by cross-sectional guides. This method has been used, for example, to model the muscular
159 components of the tails of different dinosaurs (Persons and Currie, 2011a, b; Persons et al.,
160 2013). This forms the digital analogue to the creation and sculpting of physical (clay or
161 polymer) models in order to obtain muscle forces (Rayfield et al., 2001; Mazzetta et al.,
162 2009; Blanco et al., 2012).

163 The majority of muscle reconstructions are nearly entirely performed on the basis of
164 preserved hard tissues, which might not be able to provide sufficient information for unusual
165 muscle morphologies, such as muscle asymmetry, pathway curvature, or tendinous
166 attachments. Similarly, fascia, tendons, and ligaments are rarely preserved in fossil taxa
167 (Organ and Adams, 2005; Organ, 2006) but may form an important functional component. It
168 is therefore advisable to interpret osteological correlates and emanating reconstruction in the
169 context of living taxa (Fig. 2E). By employing an extant phylogenetic bracket approach
170 (Witmer, 1995), homologies for muscle position and arrangement can be established.
171 Furthermore, novel imaging techniques, such as contrast-enhanced CT scanning (Metscher,
172 2009; Lautenschlager et al., 2014a; Gignac et al., 2016), magnetic resonance imaging (Sharp
173 and Trusler, 2015), or phase-contrast CT scanning (Walsh et al., 2013b), can provide further
174 information and comparative data.

175

176

ENDOCRANIAL ANATOMY

177 **Examples**

178 The study of the endocranial anatomy, including the brain, inner ear, and
179 neurovascular structures (i.e., nerves, blood vessels), of fossil animals has a long-standing
180 history in paleontological research (Marsh, 1885; Edinger, 1929; Hopson, 1979; Buchholtz
181 and Seyfarth, 1999, 2001). Due to the poor preservation potential of soft-tissue structures,
182 however, early researchers had to rely on a few exceptionally preserved fossil endocasts –
183 naturally occurring casts of the endocranial cavity, which are partially representative of the
184 gross anatomy of the brain and associated structures – or to prepare artificial endocasts
185 through serial grinding or casting techniques (Cunningham et al., 2014). The advent of non-
186 destructive imaging techniques has revolutionized the field of paleoneurology and facilitated
187 the acquisition and study of digital endocasts (Fig. 1B) to gain insight into brain anatomy,
188 development, and neurosensory function.

189 Since one of the first applications of CT to reconstruct the endocranial anatomy of
190 *Tyrannosaurus rex* (Brochu, 2000), the increasing availability of CT scanning technology and
191 processing software has led to a surge of digital endocast reconstructions. In the past decade,
192 digital endocasts have been created and studied for numerous fossil (and also extant) taxa
193 across all vertebrate clades, including: jawless (Gai et al., 2011) and ray-finned fish (Giles
194 and Friedman, 2014), dinosaurs (Witmer and Ridgely, 2009; Lautenschlager et al., 2012),
195 pseudosuchians (Holloway et al., 2013; von Baczko and Desojo, 2016), crocodylians (Witmer
196 et al., 2008), fossil flying and marine reptiles (Witmer et al., 2003; Marek et al., 2015), turtles
197 (Carabajal et al., 2013), birds (Ksepka et al., 2012; Balanoff et al., 2013), mammals (Rowe et
198 al., 2011; Racicot and Rowe, 2014; Ruf et al., 2016), and hominids (Zollikofer et al., 2005).
199 These and comparable studies have consequently allowed the characterization of the
200 endocranial anatomy of individual fossil taxa and provide a steadily increasing anatomical
201 resource. Furthermore, they have paved the way for large-scale comparative studies, for
202 example to shed light on the evolution of olfactory acuity in dinosaurs and birds (Zelenitsky

203 et al., 2011), deducing auditory capabilities in reptiles and birds (Walsh et al., 2009, 2013a),
204 and brain evolution across the cynodont-mammal transition (Rowe et al., 2011).

205

206 **Methodological approach**

207 Very recently, Balanoff et al. (2015) published a detailed guide on the digital
208 reconstruction of endocasts and the reader is referred to this work for an in-depth step-by-step
209 workflow. Here, a general overview on the methodological approach and potential
210 applications is provided. More details on the tomographic segmentation processes and best
211 practices can further be found in Abel et al. (2012) and Sutton et al. (2014).

212 Since digital endocasts are virtual casts of endocranial cavities enclosed by bone or
213 cartilage, their reconstruction generally requires a tomographic dataset of the studied
214 specimen. Although serial grinding methods have been used in the past and are still employed
215 for specimens with poor internal contrast (Sutton, 2008; Cunningham et al., 2014; Balanoff et
216 al., 2015), CT scanning is routinely used to obtain the necessary data. For disarticulated or
217 broken specimens, surface-scanning methods can also be used (with limitations) to
218 reconstruct parts of the endocranial anatomy (Lautenschlager and Hübner, 2013; Balanoff et
219 al., 2015). Different approaches exist as to how the endocranial components can be
220 reconstructed from the dataset. The most common one is the selection of features-of-interest
221 (e.g., endocranial cavity, bony canals of nerves) in subsequent tomographic slices – a process
222 known as segmenting or labelling (Fig. 3A). Depending on the quality of the dataset, this can
223 be done semi-automatically on the basis of a specific greyscale value, which represents the
224 cranial cavities and separates them from the bony housing. For fossil specimens, however,
225 this is often not possible where sedimentary matrix has infilled the endocranial cavities and
226 fossilization processes have remineralized the bone. As a result, the density of the matrix and
227 (remineralized) hard tissues and their respective grey scale values are often too similar to

228 define a distinct threshold. In such cases, segmentation has to be performed manually by
229 tracing the boundary of the features-of-interest. Once the complete dataset or region-of-
230 interest has been segmented, the individual slice labels are used to calculate a 3-D surface
231 (Fig. 3B, C). A variety of software exists (Cunningham et al., 2014; Balanoff et al., 2015) for
232 the segmentation and visualization of digital endocasts, ranging from freely available
233 programs, such as SPIERS (Sutton et al., 2012) and Drishti
234 (<http://sf.anu.edu.au/Vizlab/drishti/index.shtml>), to commercial products, including Avizo
235 (VSG, Visualisation Science Group), Mimics (Materialise) and VG Studio Max (Volume
236 Graphics). The programs can differ considerably in the types of segmentation and image
237 processing tools, import and export capabilities, and visualization quality, and the choice
238 mostly depends on availability and personal preference.

239

240

OTHER CRANIAL SOFT TISSUES

Examples

242 Apart from muscles, the brain, and neurovascular structures, a number of other soft-
243 tissues occupy the cranial skeleton. Of these, not all have been nor can be reconstructed in
244 fossils as they leave no or only weak osteological correlates. A few examples exist for
245 various other cranial soft tissue reconstructions.

246 Cranial pneumatic sinuses are among the most commonly reconstructed structures not
247 pertaining to musculature or the endocranial anatomy (Fig. 1C). These sinuses represent
248 pneumatic invasions of air-filled epithelial diverticula, leaving distinct cavities in the bone.
249 They have been reconstructed for a number of dinosaurian taxa (Kundrát and Janáček, 2007;
250 Tahara and Larsson, 2011; Gold et al., 2013) and other archosaurs (Witmer and Ridgely,
251 2008), marine mammals (Racicot and Rowe, 2014), and hominids (Zollikofer et al., 2008).

252 Similarly, the bony nasal cavity of vertebrates is filled by a number of different soft-
253 tissue structures, such as cartilaginous conchae (turbinates) and epithelia. Although
254 osteological correlates are rarely preserved, different conchae morphologies have been
255 reconstructed in an ornithischian dinosaur using information from computational fluid
256 dynamics modelling (Bourke et al., 2015).

257 Further examples include keratinous structures covering bony surfaces, such as beak-
258 like rhamphothecae of theropod dinosaurs. Based on osteological inferences, such keratinous
259 sheaths have been reconstructed in different theropods (Lautenschlager et al., 2013;
260 Lautenschlager et al., 2014b; Cuff and Rayfield, 2015).

261

262 **Methodological approach**

263 Due to the variety of different cranial soft-tissues, reconstruction methods differ with
264 and depending on the type of soft-tissue. The reconstruction process of cranial pneumatic
265 sinuses is largely comparable to that of the endocranial anatomy. As many pneumatic sinuses
266 are nearly completely enclosed by bone, tomographic datasets are necessary. An exception
267 are the sinuses that occupy external regions, such as the antorbital sinus of archosaurs, for the
268 reconstruction of which surface scans can suffice. Following the digitization (and if necessary
269 conversion into a tomographic dataset) of the specimen, cavities representing sinuses are
270 segmented and subsequently visualized. For pneumatic sinuses covering parts of the external
271 surfaces, boundaries might not be clearly constrained. The recommended approach in these
272 cases is to create a reconstruction flush with the margins of the surrounding bone structure.

273 For soft-tissues covering the external surface of bones, such as keratinous structures, a
274 similar approach can be applied. Both tomographic and surface-scan datasets can be used, as
275 no internal features are relevant for the reconstruction. However, this poses another problem.
276 As surface features only constrain the location and extent of a keratinous sheath, its thickness

277 and external boundaries are not constrained by hard-tissues. This information has to be
278 obtained from comparisons with extant taxa forming a phylogenetic bracket. For example,
279 data on the thickness and arrangement of the rhamphotheca of extant birds can be used to
280 inform reconstructions in fossils (Soons et al., 2012; Lautenschlager et al., 2013).

281 In cases, where preserved hard-tissues do not offer any constraints on the shape and
282 position of soft-tissues, a hypotheses-testing approach may be applied using computational
283 models. To reconstruct the morphology and position of conchae within the nasal capsule of
284 an ornithischian dinosaur, Bourke et al., (2015) used computational fluid dynamics to test
285 airflow for varying configurations. Different models of conchae, as found in extant taxa, were
286 created in the 3-D modelling and visualization software Maya (Autodesk Inc.) and their effect
287 on inspiratory airflow were tested virtually. This allowed the identification of the most likely
288 morphology and arrangement of the soft-tissue conchae in spite of the absence of osteological
289 correlates.

290

291 **WHOLE-BODY AND LIFE RECONSTRUCTIONS**

292 **Examples**

293 As shown above, the majority of soft-tissue reconstructions are focussed on a
294 particular anatomical structure or skeletal region. However, knowledge on the whole-body
295 soft-tissue morphology can be necessary to address question about body mass evolution,
296 locomotory performance, and paleoecology (e.g., Allen et al., 2013; Maidment et al., 2014).
297 Virtual whole-body reconstructions have been created of placoderms (Bécharde et al., 2014),
298 early tetrapods (Nyakatura et al., 2015), various dinosaurs (Gunga et al., 2007; Hutchinson et
299 al., 2007; Ósi and Makádi, 2009), fossil birds (Brassey et al., 2016), and mammals (Brassey
300 and Gardiner, 2015), as well as invertebrates (Garwood and Dunlop, 2014). A large number

301 of these reconstructions have been created on the basis of complete skeletons in order to
302 obtain body mass estimates or to investigate locomotory behaviour.

303 In contrast, digital life reconstructions (Fig. 1D) have been created to provide
304 hypotheses regarding the appearance of extinct organisms, including fossil cephalopods
305 (Lukeneder, 2012), stegocephalians (Steyer et al., 2010), and mammals (Cherin et al., 2016).
306 Although such models are often based on preserved hard-tissues, they include a large degree
307 of interpretation and artistic license, and are mainly intended to supplement studies rather
308 than act as the focus of scientific investigation.

309

310 **Methodological approach**

311 Virtual whole-body reconstructions are usually based on digitized skeletons, but can
312 also be created using two-dimensional images as a template (see Rahman and
313 Lautenschlager, in review). Due to the large size and number of individual skeletal elements,
314 digitization is typically performed using surface-based methods such as laser scanning or
315 photogrammetry (Gunga et al., 2007; Bates et al., 2009; Mallison and Wings, 2014). For
316 fossil specimens, the digital removal of taphonomic artefacts and rearticulation of elements
317 might be necessary, before the actual whole-body reconstruction can be performed (Gunga et
318 al., 2007; Mallison, 2010).

319 Different methods exist for the subsequent reconstruction of the soft-tissue
320 morphology. To aid in the reconstruction and to increase accuracy, the digitized model is
321 usually subdivided into functional units (e.g., skull, torso, limbs). To generate the soft-tissue
322 outline, simple geometric shapes (spheres, cylinders, ellipses) are superimposed onto each
323 unit and adjusted to match and envelop the underlying shape of the skeletal elements
324 (Hutchinson et al., 2007; Bates et al., 2009; Mallison, 2010), often informed by frontal or
325 sagittal cross-section profiles (Liu et al., 2015). Additional components representing internal

326 organs, such as lungs and air sacks, can be included to improve subsequent body mass
327 estimates (Hutchinson et al., 2007; Bates et al., 2009). Similarly, variations of the individual
328 components may be created to allow for “tight-fitting” or “loose” morphologies in order to
329 provide minimum and maximum mass estimates.

330 The calculation of convex hull volumes presents an alternative to the manual
331 adjustment of the soft-tissue outlines, which inevitably introduces a certain degree of
332 interpretation into the model (Sellers et al., 2012; see also Brassey, in review). A convex hull
333 is the smallest polygon, which contains a set of given points. As such a convex hull
334 represents the minimum volume to envelop predetermined coordinates/points deemed
335 important in three-dimensional space. As it is based on mathematical calculations, the convex
336 hull method has the advantage that it can be automated using numerical computing tools such
337 as MatLab (MathWorks Inc.) and is less prone to personal interpretation. The convex hull
338 method has been applied to a variety of fossil taxa to provide body mass estimates (Brassey et
339 al., 2015; Bates et al., 2015; Brassey et al., 2016).

340 Similar to whole-body reconstructions, life reconstructions are usually based on
341 digitized fossil specimens. However, unlike the approach for whole-body reconstructions, no
342 clear sets of standards or best practices have been formulated for the creation of life
343 reconstructions. However, this is difficult to achieve considering that life reconstruction tend
344 to be scientifically informed works of art, prone to subjectivity and artistic license. Existing
345 examples (Steyer et al., 2010; Lukeneder, 2012) have used CAD and 3-D modelling
346 programs, such as Maya (Autodesk Inc.) and ZBrush (Pixologic Inc.), to create soft-tissue
347 morphologies. Several details, such as colouration, ornamentation, and the location of soft-
348 tissues, such as the external naris or the eyeball, have been created subjectively, although
349 results from other studies (e.g., Witmer, 2001; Hieronymus et al., 2009; Vinther, 2015) could

350 potentially be included to inform future reconstructions. This could add additional value to
351 life reconstructions as a useful tool for public understanding and outreach.

352

353 **LIMITATIONS AND FUTURE DIRECTIONS**

354 Digital approaches offer a huge potential to reconstruct soft-tissue structures of fossil
355 organisms. However, their accuracy depends greatly on the presence and quality of preserved
356 hard-tissues. Taphonomic artefacts, pathologies, ontogeny, and intraspecific variation can
357 present major challenges during the reconstruction process. In addition, the method used to
358 digitize specimens and the quality (e.g., scan resolution, model size, digital artefacts) of the
359 resulting models can affect the ability to identify osteological correlates and other
360 information necessary for the reconstruction process. It is therefore recommended to obtain
361 and compare information from physical specimens and the corresponding digital
362 representations. Furthermore, clear and traceable documentation of the digitization, hard-
363 tissue restorations (if performed), and the soft-tissue reconstruction should be provided so
364 that other researchers are in a position to evaluate the results or to adjust models, if new
365 information comes to light.

366 In the past, concerns have been raised when reconstructing soft-tissues in fossils
367 (McGowan, 1979; Brown, 1981; Bryant and Seymour, 1990). Not all soft-tissue structures,
368 such as muscles, will necessarily leave osteological correlates, whereas other osteological
369 correlates might not relate to the presence of the presumed soft-tissues (McGowan, 1982;
370 Nicholls and Russell, 1985). This problem not only pertains to digital reconstruction in
371 particular, but soft-tissue interpretations in paleontological studies in general. As suggested
372 above, phylogenetically informed reconstructions making use of extant taxa can help
373 minimize erroneous identifications (Bryant and Russell, 1992; Witmer, 1995). Similarly,

374 information obtained from different sources, for example different specimens, analytical
375 methods, and sensitivity tests can help to constrain and refine soft-tissue reconstructions.

376 Further limitations exist for the reconstruction of soft-tissues that are not or only
377 partially constrained by hard-tissues, as for example the extent and external boundaries of
378 muscles. Where possible, it is recommended to create such reconstructions flush with the
379 surrounding hard-tissues to avoid unnatural bulges and extreme morphologies. For some soft-
380 tissues, including the appendicular musculature, this approach can rarely be applied and the
381 extant phylogenetic bracket approach is recommended here as the best solution.

382 Further concern has been raised that digital soft-tissue reconstructions are not reliable
383 representations of the in-vivo condition (Jerison, 1973). In particular, the relationship
384 between endocranial casts and the actual brain morphology has been discussed. Due to the
385 presence of other soft-tissues, such as the dural meninges, vascular structures, and pneumatic
386 sinuses, a cast of the endocranial cavity might not necessarily represent the actual brain. The
387 degree to which an endocast reflects brain morphology can vary across different vertebrate
388 clades (Hopson, 1979; Hurlburt et al., 2013; Balanoff et al., 2015). However, the combination
389 of novel digital techniques and close comparisons with a range of extant taxa can provide an
390 important step towards a solution to this problem. By using homologous osteological
391 correlates, more accurate approximations of anatomical brain regions have been created
392 (Morhardt et al., 2012). This offers a promising approach for future studies.

393 Similarly, the use of biomechanical modelling techniques, such as FEA, MDA, or
394 CFD, provides future avenues to test soft-tissue reconstructions and competing hypotheses
395 (e.g., Bourke et al., 2015). The integration of different soft-tissue structures could further be
396 used to constrain and inform reconstructions. So far, soft-tissue reconstructions have mostly
397 focussed on individual structures, such as muscles or the endocranial anatomy. However,
398 using such existing reconstructions could provide additional information when reconstructing

399 additional features (e.g., three-dimensional models of the cranial musculature can be used to
400 constrain the position of the eyeball).

401 The surge of digital techniques has ushered in a large increase in digital soft-tissue
402 reconstructions over the past decade. However, to date the largest disadvantages are the
403 amount of time required to perform digital reconstructions, the financial cost involved to
404 purchase hardware and software licenses, and the degree of interpretation and subjectivity
405 introduced into the models due to the often manual approaches. A key prospect for the future
406 will therefore lie in the automation of reconstructions. Methods, such as convex hull mass
407 estimates (see above) or the use of geometric morphometrics to restore hominid crania (Gunz
408 et al., 2009; Gunz, 2015; Senck et al., 2015) have incorporated automation into the
409 reconstruction process, thereby minimizing individual subjectivity and providing increased
410 reproducibility.

411

412

CONCLUDING REMARKS

413 Detailed knowledge on soft-tissue structures is paramount to understanding the
414 paleobiology, paleoecology, and phylogeny of fossil organisms. Although rarely preserved,
415 recent advances in digital imaging and modelling techniques provide versatile tools to
416 reconstruct different soft-tissue structures. Using the methods presented and reviewed here, it
417 is possible to reconstruct, for example, the cranial and postcranial musculature of dinosaurs,
418 the endocranial (brain and inner ear) anatomy of early mammals and their kin, and the body
419 mass of different tetrapods from whole-body reconstructions. Because such reconstructions
420 are performed on the basis of preserved hard-tissues, they have nearly exclusively focussed
421 on vertebrate fossils in the past, although many of the techniques are also applicable to
422 invertebrate fossils. However, this also means that the quality and accuracy of the
423 reconstructed soft-tissues depends to a considerable degree on the presence and preservation

424 of hard-tissues. Consequently, the restoration of osteological-based models and the removal
425 of preservational artefacts should be performed before any soft-tissue reconstructions are
426 attempted. To avoid further uncertainties regarding the presence of osteological correlates
427 and possible homologies, it is recommended that all reconstructions are performed in a
428 phylogenetically ground framework using an extant phylogenetic bracket approach. Although
429 some uncertainties and interpretation are inevitably introduced in the reconstruction process,
430 soft-tissue reconstructions are nevertheless worthwhile as they allow researchers to gain
431 useful approximations and estimates of fossil properties, which could not be assessed
432 otherwise. Due to the digital nature of the reconstructions, it is possible to export the
433 information to other applications (e.g., FEA, MDA) to test different competing hypotheses. It
434 is anticipated that further technological advances will allow automation of certain steps,
435 enabling large-scale comparative studies and increased objectivity.

436

437

ACKNOWLEDGMENTS

438 Imran Rahman (Oxford University Museum of Natural History) and Leif Tapanila (Idaho
439 State University, Idaho Museum of Natural History) are thanked for the opportunity to
440 contribute to this edition. Lawrence Witmer (Ohio University) kindly provided additional
441 images used in Figure 1.

442

REFERENCES

443 ABEL, R. L., C. R. LAURINI, and M. RICHTER. 2012. A palaeobiologist's guide to

444 'virtual' micro-CT preparation. *Palaeontologia Electronica*, 15(2):6T.

445 ADAMS, L. A. 1918. A memoir on the phylogeny of the jaw muscles in recent and fossil

446 vertebrates. *Annals of the New York Academy of Sciences*, 28(1):51–166.

447 ALLEN, V., K. T. BATES, Z. LI, and J. R. HUTCHINSON. 2013. Linking the evolution of

448 body shape and locomotor biomechanics in bird-line archosaurs. *Nature*,

449 497(7447):104–107.

450 ALLISON, P. A., and D. E. G. BRIGGS. 1993. Exceptional fossil record: Distribution of

451 soft-tissue preservation through the Phanerozoic. *Geology*, 21(6):527–530.

452 BALANOFF, A. M., G. BEVER, M. W. COLBERT, J. A. CLARKE, D. J. FIELD, P. M.

453 GIGNAC, D. T. KSEPKA, R. C. RIDGELY, N. A. SMITH, C. R. TORRES, S.

454 WALSH, and L. M. WITMER. 2015. Best practices for digitally constructing

455 endocranial casts: examples from birds and their dinosaurian relatives. *Journal of*

456 *Anatomy*: Online before print.

457 BALANOFF, A. M., G. S. BEVER, T. B. ROWE, and M. A. NORELL. 2013. Evolutionary

458 origins of the avian brain. *Nature*, 501(7465):93–96.

459 BARGHUSEN, H. R. 1973. The adductor jaw musculature of *Dimetrodon* (Reptilia,

460 Pelycosauria). *Journal of Paleontology*, 47:823–834.

461 BATES, K. T., and P. L. FALKINGHAM. 2012. Estimating maximum bite performance in

462 *Tyrannosaurus rex* using multi-body dynamics. *Biology Letters*, 8:20120056.

463 BATES, K. T., P. L. FALKINGHAM, S. MACAULAY, C. BRASSEY, and S. C. R.

464 MAIDMENT. 2015. Downsizing a giant: re-evaluating *Dreadnoughtus* body mass.

465 *Biology Letters*, 11:20150215.

466 BATES, K. T., P. L. MANNING, D. HODGETTS, and W. I. SELLERS. 2009. Estimating
467 mass properties of dinosaurs using laser imaging and 3D computer modelling. *PLoS*
468 *one*, 4(2):e4532.

469 BÉCHARD, I., F. ARSENAULT, R. CLOUTIER, and J. KERR. 2014. The Devonian
470 placoderm fish *Bothriolepis canadensis* revisited with three-dimensional digital
471 imagery. *Palaeontologia Electronica*, 17(1):1–19.

472 BERNARD, S., K. BENZERARA, O. BEYSSAC, N. MENGUY, F. GUYOT, G. E.
473 BROWN JR, and B. GOFFÉ. 2007. Exceptional preservation of fossil plant spores in
474 high-pressure metamorphic rocks. *Earth and Planetary Science Letters*, 262(1–2):257–
475 272.

476 BLANCO, R. E., A. RINDERKNECHT, and G. LECUONA. 2012. The bite force of the
477 largest fossil rodent (Hystricognathi, Caviomorpha, Dinomyidae). *Lethaia*, 45(2):157–
478 163.

479 BOURKE, J. M., W. M. RUGER PORTER, R. C. RIDGELY, T. R. LYSON, E. R.
480 SCHACHNER, P. R. BELL, and L. M. WITMER. 2015. Breathing life into
481 dinosaurs: tackling challenges of soft-tissue restoration and nasal airflow in extinct
482 species. *The Anatomical Record*, 297(11):2148–2186.

483 BRASSEY, C. A. In review. Body mass estimation in paleontology: a review of volumetric
484 techniques. In L. TAPANILA and I. A. RAHMAN (eds.), *Virtual Paleontology*. The
485 Paleontological Society Papers, XX.

486 BRASSEY, C. A., and J. D. GARDINER. 2015. An advanced shape-fitting algorithm applied
487 to quadrupedal mammals: improving volumetric mass estimates. *Royal Society Open*
488 *Science*, 2(8):150302.

489 BRASSEY, C. A., S. C. R. MAIDMENT, and P. M. BARRETT. 2015. Body mass estimates
490 of an exceptionally complete *Stegosaurus* (Ornithischia: Thyreophora): comparing

491 volumetric and linear bivariate mass estimation methods. *Biology Letters*, 11(3):
492 20140984

493 BRASSEY, C. A., T. G. O'MAHONEY, A. C. KITCHENER, P. L. MANNING, and W. I.
494 SELLERS. 2016. Convex-hull mass estimates of the dodo (*Raphus cucullatus*):
495 application of a CT-based mass estimation technique. *PeerJ*, 4:e1432.

496 BRIGHT, J. A. 2014. A review of paleontological finite element models and their validity.
497 *Journal of Paleontology*, 88(4):760–769.

498 BROCHU, C. A. 2000. A digitally-rendered endocast for *Tyrannosaurus rex*. *Journal of*
499 *Vertebrate Paleontology*, 20(1):1–6.

500 BROWN, D. S. 1981. The English Upper Jurassic Plesiosauroidea (Reptilia) and a review of
501 the phylogeny and classification of the Plesiosauria. *Bulletin of the British Museum*
502 (Natural History), *Geology*, 35:253–347.

503 BRYANT, H. N., and A. P. RUSSELL. 1992. The role of phylogenetic analysis in the
504 inference of unpreserved attributes of extinct taxa. *Philosophical Transactions of the*
505 *Royal Society of London B: Biological Sciences*, 337(1282):405–418.

506 BRYANT, H. N., and K. L. SEYMOUR. 1990. Observations and comments on the reliability
507 of muscle reconstruction in fossil vertebrates. *Journal of Morphology*, 206(1):109–
508 117.

509 BUCHHOLTZ, E. A., and E.-A. SEYFARTH. 1999. The gospel of the fossil brain: Tilly
510 Edinger and the science of paleoneurology. *Brain Research Bulletin*, 48(4):351–361.

511 BUCHHOLTZ, E. A., and E.-A. SEYFARTH. 2001. The study of “fossil brains”: Tilly
512 Edinger (1897–1967) and the beginnings of paleoneurology. *BioScience*, 51(8):674–
513 682.

514 BUDD, G. E. 1998. Arthropod body-plan evolution in the Cambrian with an example from
515 anomalocaridid muscle. *Lethaia*, 31(3):197–210.

516 BUTTERFIELD, N. J. 2003. Exceptional fossil preservation and the Cambrian explosion.
517 Integrative and Comparative Biology, 43(1):166–177.

518 BUTTON, D. J., E. J. RAYFIELD, and P. M. BARRETT. 2014. Cranial biomechanics
519 underpins high sauropod diversity in resource-poor environments. Proceedings of the
520 Royal Society of London B: Biological Sciences, 281(1795):20142114.

521 CARABAJAL, A. P., J. STERLI, J. MÜLLER, and A. HILGER. 2013. Neuroanatomy of the
522 Marine Jurassic Turtle *Plesiochelys etalloni* (Testudinata, Plesiochelyidae). PloS one,
523 8(7):e69264.

524 CHAPMAN, T., F. MOISEEV, V. SHOLUKHA, S. LOURYAN, M. ROOZE, P. SEMAL,
525 and S. V. S. JAN. 2010. Virtual reconstruction of the Neandertal lower limbs with an
526 estimation of hamstring muscle moment arms. Comptes Rendus Palevol, 9(6):445–
527 454.

528 CHERIN, M., D. A. IURINO, R. SARDELLA, and L. ROOK. 2014. *Acinonyx pardinensis*
529 (Carnivora, Felidae) from the Early Pleistocene of Pantalla (Italy): predatory behavior
530 and ecological role of the giant Plio–Pleistocene cheetah. Quaternary Science
531 Reviews, 87:82–97.

532 CHERIN, M., D. A. IURINO, G. WILLEMSSEN, and G. CARNEVALE. 2016. A new otter
533 from the Early Pleistocene of Pantalla (Italy), with remarks on the evolutionary
534 history of Mediterranean Quaternary Lutrinae (Carnivora, Mustelidae). Quaternary
535 Science Reviews, 135:92–102.

536 CUFF, A. R., and E. J. RAYFIELD. 2015. Retrodeformation and muscular reconstruction of
537 ornithomimosaurian dinosaur crania. PeerJ, 3:e1093.

538 CUNNINGHAM, J. A., I. A. RAHMAN, S. LAUTENSCHLAGER, E. J. RAYFIELD, and P.
539 C. J. DONOGHUE. 2014. A virtual world of paleontology. Trends in Ecology &
540 Evolution, 29(6):347–357.

541 CURTIS, N. 2011. Craniofacial biomechanics: an overview of recent multibody modelling
542 studies. *Journal of Anatomy*, 218(1):16–25.

543 CURTIS, N., K. KUPCZIK, P. O'HIGGINS, M. MOAZEN, and M. FAGAN. 2008.
544 Predicting skull loading: applying multibody dynamics analysis to a macaque skull.
545 *The Anatomical Record*, 291(5):491–501.

546 DILKES, D. W. 1999. Appendicular myology of the hadrosaurian dinosaur *Maiasaura*
547 *peeblesorum* from the Late Cretaceous (Campanian) of Montana. *Earth and*
548 *Environmental Science Transactions of the Royal Society of Edinburgh*, 90(2):87–
549 125.

550 DILKES, D. W., J. R. HUTCHINSON, C. M. HOLLIDAY, and L. M. WITMER. 2012.
551 Reconstructing the musculature of dinosaurs, p. 151–190. *In* M. K. BRETT-
552 SURMAN, T. R. HOLTZ, and J. O. FARLOW (eds.), *The Complete Dinosaur*.
553 Indiana University Press, Bloomington, IN.

554 DUMONT, E., I. R. GROSSE, and G. J. SLATER. 2009. Requirements for comparing the
555 performance of finite element models of biological structures. *Journal of Theoretical*
556 *Biology*, 256(1):96–103.

557 EDINGER, T. 1929. Die fossilen Gehirne. *Ergebnisse der Anatomie und*
558 *Entwicklungsgeschichte*, 28:1–249.

559 FOFFA, D., A. R. CUFF, J. SASSOON, E. J. RAYFIELD, M. N. MAVROGORDATO, and
560 M. J. BENTON. 2014. Functional anatomy and feeding biomechanics of a giant
561 Upper Jurassic pliosaur (Reptilia: Sauropterygia) from Weymouth Bay, Dorset, UK.
562 *Journal of Anatomy*, 225(2):209–219.

563 FREY, E., D. M. MARTILL, and M.-C. BUCHY. 2003. A new species of tapejarid pterosaur
564 with soft-tissue head crest. *Geological Society, London, Special Publications*,
565 217(1):65–72.

566 GAI, Z., P. C. DONOGHUE, M. ZHU, P. JANVIER, and M. STAMPANONI. 2011. Fossil
567 jawless fish from China foreshadows early jawed vertebrate anatomy. *Nature*,
568 476(7360):324–327.

569 GARWOOD, R., and J. DUNLOP. 2014. The walking dead: Blender as a tool for
570 paleontologists with a case study on extinct arachnids. *Journal of Paleontology*,
571 88(04):735–746.

572 GERRIENNE, P., D. L. DILCHER, S. BERGAMASCHI, I. MILAGRES, E. PEREIRA, and
573 M. A. C. RODRIGUES. 2006. An exceptional specimen of the early land plant
574 *Cooksonia paranensis*, and a hypothesis on the life cycle of the earliest
575 eutracheophytes. *Review of Palaeobotany and Palynology*, 142(3–4):123–130.

576 GIGNAC, P. M., N. J. KLEY, J. A. CLARKE, M. W. COLBERT, A. C. MORHARDT, D.
577 CERIO, I. N. COST, P. G. COX, J. D. DAZA, and C. M. EARLY. 2016. Diffusible
578 iodine-based contrast-enhanced computed tomography (diceCT): an emerging tool for
579 rapid, high-resolution, 3-D imaging of metazoan soft tissues. *Journal of Anatomy*.
580 Online before print.

581 GILES, S., and M. FRIEDMAN. 2014. Virtual reconstruction of endocast anatomy in early
582 ray-finned fishes (Osteichthyes, Actinopterygii). *Journal of Paleontology*, 88(4):636–
583 651.

584 GOLD, M. E. L., S. L. BRUSATTE, and M. A. NORELL. 2013. The cranial pneumatic
585 sinuses of the tyrannosaurid *Alioramus* (Dinosauria: Theropoda) and the evolution of
586 cranial pneumaticity in theropod dinosaurs. *American Museum Novitates*. 3790:1–46.

587 GROSSE, I. R., E. R. DUMONT, C. COLETTA, and A. TOLLESON. 2007. Techniques for
588 modelling muscle-induced forces in finite element models of skeletal structures. *The*
589 *Anatomical Record*, 290(9):1069–1088.

590 GUNGA, H.-C., T. SUTHAU, A. BELLMANN, A. FRIEDRICH, T. SCHWANEBECK, S.
591 STOINSKI, T. TRIPPEL, K. KIRSCH, and O. HELLWICH. 2007. Body mass
592 estimations for *Plateosaurus engelhardti* using laser scanning and 3D reconstruction
593 methods. *Naturwissenschaften*, 94(8):623–630.

594 GUNZ, P. 2015. Computed tools for paleoneurology, p. 39–55, *Human Paleoneurology*.
595 Springer International Publishing.

596 GUNZ, P., P. MITTEROECKER, S. NEUBAUER, G. W. WEBER, and F. L. BOOKSTEIN.
597 2009. Principles for the virtual reconstruction of hominin crania. *Journal of Human*
598 *Evolution*, 57(1):48–62.

599 HIERONYMUS, T. L., L. M. WITMER, D. H. TANKE, and P. J. CURRIE. 2009. The facial
600 integument of centrosaurine ceratopsids: morphological and histological correlates of
601 novel skin structures. *The Anatomical Record*, 292(9):1370–1396.

602 HOLLIDAY, C. M. 2009. New insights into dinosaur jaw muscle anatomy. *The Anatomical*
603 *Record*, 292:1246–1265.

604 HOLLOWAY, W. L., K. M. CLAESON, and F. R. O’KEEFE. 2013. A virtual phytosaur
605 endocast and its implications for sensory system evolution in archosaurs. *Journal of*
606 *Vertebrate Paleontology*, 33(4):848–857.

607 HOPSON, J. 1979. Paleoneurology, p. 39–146. *In* C. GANS (ed.), *Biology of the*
608 *Reptilia*. Volume 9. Academic Press, London.

609 HURLBURT, G. R., R. C. RIDGELY, and L. M. WITMER. 2013. Relative size of brain and
610 cerebrum in tyrannosaurid dinosaurs: an analysis using brain-endocast quantitative
611 relationships in extant alligators, p. 1–21. *In* J. M. PARRISH, R. E. MOLNAR, P. J.
612 CURRIE, and E. B. KOPPELHUS (eds.), *Tyrannosaurid Paleobiology*. Indiana
613 University Press, Bloomington.

614 HUTCHINSON, J. R., F. C. ANDERSON, S. S. BLEMKER, and S. L. DELP. 2005.
615 Analysis of hindlimb muscle moment arms in *Tyrannosaurus rex* using a three-
616 dimensional musculoskeletal computer model: implications for stance, gait, and
617 speed. *Paleobiology*, 31(4):676–701.

618 HUTCHINSON, J. R., V. NG-THOW-HING, and F. C. ANDERSON. 2007. A 3D
619 interactive method for estimating body segmental parameters in animals: application
620 to the turning and running performance of *Tyrannosaurus rex*. *Journal of Theoretical*
621 *Biology*, 246(4):660–680.

622 JERISON, H. 1973. *Evolution of the Brain and Intelligence*. Academic Press, New York.

623 KSEPKA, D. T., A. M. BALANOFF, S. WALSH, A. REVAN, and A. HO. 2012. Evolution
624 of the brain and sensory organs in Sphenisciformes: new data from the stem penguin
625 *Paraptendytes antarcticus*. *Zoological Journal of the Linnean Society*, 166(1):202–
626 219.

627 KUNDRÁT, M., and J. JANÁČEK. 2007. Cranial pneumatization and auditory perceptions
628 of the oviraptorid dinosaur *Conchoraptor gracilis* (Theropoda, Maniraptora) from the
629 Late Cretaceous of Mongolia. *Naturwissenschaften*, 94(9):769–778.

630 LAUTENSCHLAGER, S. 2012. *Paleontology 2.0 – A comprehensive protocol for the*
631 *reconstruction of hard- and soft tissue structures in fossils*. *Geological Society of*
632 *America Program and Abstracts*, 44:372.

633 LAUTENSCHLAGER, S. 2013. Cranial myology and bite force performance of
634 *Erlikosaurus andrewsi*: A novel approach for digital muscle reconstructions. *Journal*
635 *of Anatomy*, 222(2):260–272.

636 LAUTENSCHLAGER, S. 2015. Estimating cranial musculoskeletal constraints in theropod
637 dinosaurs. *Royal Society Open Science*, 2(11):150495.

638 LAUTENSCHLAGER, S., J. A. BRIGHT, and E. J. RAYFIELD. 2014a. Digital dissection–
639 using contrast-enhanced computed tomography scanning to elucidate hard-and soft-
640 tissue anatomy in the Common Buzzard *Buteo buteo*. *Journal of Anatomy*,
641 224(4):412–431.

642 LAUTENSCHLAGER, S., and T. HÜBNER. 2013. Ontogenetic trajectories in the
643 ornithischian endocranium. *Journal of evolutionary biology*, 26(9):2044–2050.

644 LAUTENSCHLAGER, S., E. J. RAYFIELD, P. ALTANGEREL, L. E. ZANNO, and L. M.
645 WITMER. 2012. The endocranial anatomy of Therizinosauria and its implications for
646 sensory and cognitive function. *PloS one*, 7(12):e52289.

647 LAUTENSCHLAGER, S., L. M. WITMER, P. ALTANGEREL, and E. J. RAYFIELD.
648 2013. Edentulism, beaks, and biomechanical innovations in the evolution of theropod
649 dinosaurs. *Proceedings of the National Academy of Sciences*, 110(51):20657–20662.

650 LAUTENSCHLAGER, S., L. M. WITMER, P. ALTANGEREL, L. E. ZANNO, and E. J.
651 RAYFIELD. 2014b. Cranial anatomy of *Erlikosaurus andrewsi* (Dinosauria,
652 Therizinosauria): new insights based on digital reconstruction. *Journal of Vertebrate*
653 *Paleontology*, 34(6):1263–1291.

654 LIU, J., J. SHI, L. C. FITTON, R. PHILLIPS, P. O’HIGGINS, and M. J. FAGAN. 2012. The
655 application of muscle wrapping to voxel-based finite element models of skeletal
656 structures. *Biomechanics and Modeling in Mechanobiology*, 11(1–2):35–47.

657 LIU, S., A. S. SMITH, Y. GU, J. TAN, C. K. LIU, and G. TURK. 2015. Computer
658 simulations imply forelimb-dominated underwater flight in plesiosaurs. *PLoS*
659 *Computational Biology* 11(12):e1004605.

660 LUKENEDER, A. 2012. Computed 3D visualisation of an extinct cephalopod using
661 computer tomographs. *Computers & Geosciences*, 45:68–74.

662 MAIDMENT, S. C., D. M. HENDERSON, and P. M. BARRETT. 2014. What drove
663 reversions to quadrupedality in ornithischian dinosaurs? Testing hypotheses using
664 centre of mass modelling. *Naturwissenschaften*, 101(11):989–1001.

665 MALLISON, H. 2010. The digital *Plateosaurus* I: body mass, mass distribution, and posture
666 assessed using CAD and CAE on a digitally mounted complete skeleton.
667 *Palaeontologia Electronica*, 13(13.2):1–26.

668 MALLISON, H., and O. WINGS. 2014. Photogrammetry in paleontology – a practical guide.
669 *Journal of Paleontological Techniques*, 12:1–31.

670 MAREK, R. D., B. C. MOON, M. WILLIAMS, and M. J. BENTON. 2015. The skull and
671 endocranium of a Lower Jurassic ichthyosaur based on digital reconstructions.
672 *Palaeontology*, 58(4):723–742.

673 MARSH, O. C. 1885. The gigantic mammals of the Order Dinocerata, p. 34–302, Fifth
674 Annual Report of the United States Geological Survey Washington (DC). US
675 Government Printing Office.

676 MAZZETTA, G. V., A. P. CISILINO, R. E. BLANCO, and N. CALVO. 2009. Cranial
677 mechanics and functional interpretation of the horned carnivorous dinosaur
678 *Carnotaurus sastrei*. *Journal of Vertebrate Paleontology*, 29(3):822–830.

679 MCGOWAN, C. 1979. The hind limb musculature of the brown kiwi, *Apteryx australis*
680 *mantelli*. *Journal of Morphology*, 160(1):33–73.

681 MCGOWAN, C. 1982. The wing musculature of the Brown Kiwi *Apteryx australis mantelli*
682 and its bearings on ratite affinities. *Journal of Zoology*, 197:173–219.

683 METSCHER, B. D. 2009. MicroCT for comparative morphology: simple staining methods
684 allow high-contrast 3D imaging of diverse non-mineralized animal tissues. *BMC*
685 *physiology*, 9(1):1–14.

686 MINER, R. W. 1925. The pectoral limb of Eryops and other primitive tetrapods. Bulletin of
687 the American Museum of Natural History, 51(145):1924–1925.

688 MOAZEN, M., N. CURTIS, S. E. EVANS, P. O’HIGGINS, and M. J. FAGAN. 2008. Rigid-
689 body analysis of a lizard skull: Modelling the skull of *Uromastix hardwickii*. Journal
690 of Biomechanics, 41(6):1274–1280.

691 MORHARDT, A. C., R. C. RIDGLEY, and L. M. WITMER. 2012. From endocast to brain:
692 assessing brain size and structure in extinct archosaurs using gross anatomical brain
693 region approximation (GABRA). Journal of Vertebrate Paleontology, Supplement,
694 32:145.

695 NICHOLLS, E. L., and A. P. RUSSELL. 1985. Structure and function of the pectoral girdle
696 and forelimb of *Struthiomimus altus* (Theropoda: Ornithomimidae). Palaeontology,
697 28(4):643–677.

698 NYAKATURA, J. A., V. R. ALLEN, J. LAUSTRÖER, A. ANDIKFAR, M. DANCZAK,
699 H.-J. ULLRICH, W. HUFENBACH, T. MARTENS, and M. S. FISCHER. 2015. A
700 Three-dimensional skeletal reconstruction of the stem amniote *Orobates pabsti*
701 (Diadectidae): analyses of body mass, centre of mass position, and joint mobility.
702 PloS one, 10(9):e0137284.

703 O’CONNOR, P. M. 2006. Postcranial pneumaticity: An evaluation of soft-tissue influences
704 on the postcranial skeleton and the reconstruction of pulmonary anatomy in
705 archosaurs. Journal of Morphology, 267(10):1199–1226.

706 ORGAN, C. L. 2006. Thoracic epaxial muscles in living archosaurs and ornithopod
707 dinosaurs. The Anatomical Record Part A: Discoveries in Molecular, Cellular, and
708 Evolutionary Biology, 288A(7):782–793.

709 ORGAN, C. L., and J. ADAMS. 2005. The histology of ossified tendon in dinosaurs. Journal
710 of Vertebrate Paleontology, 25(3):602–613.

711 ÓSI, A., and L. MAKÁDI. 2009. New remains of *Hungarosaurus tormai* (Ankylosauria,
712 Dinosauria) from the Upper Cretaceous of Hungary: skeletal reconstruction and body
713 mass estimation. *Paläontologische Zeitschrift*, 83(2):227–245.

714 PERSONS IV, W. S., and P. J. CURRIE. 2011a. Dinosaur speed demon: the caudal
715 musculature of *Carnotaurus sastrei* and implications for the evolution of South
716 American abelisaurids. *PloS one*, 6(10):e25763.

717 PERSONS IV, W. S., and P. J. CURRIE. 2011b. The tail of *Tyrannosaurus*: reassessing the
718 size and locomotive importance of the m. caudofemoralis in non-avian theropods. *The*
719 *Anatomical Record*, 294(1):119–131.

720 PERSONS IV, W. S., P. J. CURRIE, and M. A. NORELL. 2013. Oviraptorosaur tail forms
721 and functions. *Acta Palaeontologica Polonica*, 59(3):553–567.

722 RACICOT, R. A., and T. ROWE. 2014. Endocranial anatomy of a new fossil porpoise
723 (Odontoceti, Phocoenidae) from the Pliocene San Diego Formation of California.
724 *Journal of Paleontology*, 88(04):652–663.

725 RAHMAN, I. A. and S. LAUTENSCHLAGER. In review. Applications of three-dimensional
726 box modeling to paleontological functional analysis. *In* L. TAPANILA and I. A.
727 RAHMAN (eds.), *Virtual Paleontology*. The Paleontological Society Papers, XX.

728 RAHMAN, I. A., S. ZAMORA, P. L. FALKINGHAM, and J. C. PHILLIPS. 2015. Cambrian
729 cinctan echinoderms shed light on feeding in the ancestral deuterostome. *Proceedings*
730 *of the Royal Society of London B: Biological Sciences*, 282(1818):
731 20151964. RAYFIELD, E. J. 2007. Finite Element Analysis and understanding the
732 biomechanics and evolution of living and fossil organisms. *Annual Review of Earth*
733 *and Planetary Sciences*, 35(1):541–576.

734 RAYFIELD, E. J., D. B. NORMAN, C. C. HORNER, J. R. HORNER, P. M. SMITH, J. J.
735 THOMASON, and P. UPCHURCH. 2001. Cranial design and function in a large
736 theropod dinosaur. *Nature*, 409(6823):1033–1037.

737 ROMER, A. S. 1923. The pelvic musculature of saurischian dinosaurs. *Bulletin of the*
738 *American Museum of Natural History*, 49:605–617.

739 ROWE, T. B., T. E. MACRINI, and Z.-X. LUO. 2011. Fossil evidence on origin of the
740 mammalian brain. *Science*, 332(6032):955–957.

741 RUF, I., V. VOLPATO, K. D. ROSE, G. BILLET, C. DE MUIZON, and T. LEHMANN.
742 2016. Digital reconstruction of the inner ear of *Leptictidium auderiense* (Leptictida,
743 Mammalia) and North American leptictids reveals new insight into leptictidan
744 locomotor agility. *Paläontologische Zeitschrift*:1–19. Online before print.

745 SASSO, C. D., and M. SIGNORE. 1998. Exceptional soft-tissue preservation in a theropod
746 dinosaur from Italy. *Nature*, 392(6674):383–387.

747 SCHOPF, J. M. 1975. Modes of fossil preservation. *Review of Palaeobotany and Palynology*,
748 20(1):27–53.

749 SCHWEITZER, M. H. 2011. Soft tissue preservation in terrestrial Mesozoic vertebrates.
750 *Annual Review of Earth and Planetary Sciences*, 39(1):187–216.

751 SELLERS, W., J. HEPWORTH-BELL, P. FALKINGHAM, K. BATES, C. BRASSEY, V.
752 EGERTON, and P. MANNING. 2012. Minimum convex hull mass estimations of
753 complete mounted skeletons. *Biology Letters*, 8:20120263.

754 SELLERS, W. I., L. MARGETTS, R. A. CORIA, and P. L. MANNING. 2013. March of the
755 titans: The locomotor capabilities of sauropod dinosaurs. *PloS one*, 8(10):e78733.

756 SENCK, S., F. L. BOOKSTEIN, S. BENAZZI, J. KASTNER, and G. W. WEBER. 2015.
757 Virtual reconstruction of modern and fossil hominoid crania: consequences of
758 reference sample choice. *The Anatomical Record*, 298(5):827–841.

759 SHARP, A. C. 2014. Three dimensional digital reconstruction of the jaw adductor
760 musculature of the extinct marsupial giant *Diprotodon optatum*. PeerJ, 2:e514.

761 SHARP, A. C., and P. W. TRUSLER. 2015. Morphology of the jaw-closing musculature in
762 the common wombat (*Vombatus ursinus*) using digital dissection and magnetic
763 resonance imaging. PloS one, 10(2):e0117730.

764 SNIVELY, E., J. R. COTTON, R. RIDGELY, and L. M. WITMER. 2013. Multibody
765 dynamics model of head and neck function in *Allosaurus* (Dinosauria, Theropoda).
766 Palaeontologia Electronica, 16(2):11A.

767 SOONS, J., A. HERREL, P. AERTS, and J. DIRCKX. 2012. Determination and validation of
768 the elastic moduli of small and complex biological samples: bone and keratin in bird
769 beaks. Journal of The Royal Society Interface, 9(71):1381–1388.

770 STEYER, J. S., M. BOULAY, and S. LORRAIN. 2010. 3D external restorations of
771 stegocephalian skulls using ZBrush: The renaissance of fossil amphibians. Comptes
772 Rendus Palevol, 9(6):463–470.

773 SUMIDA, S. S. 1989. The appendicular skeleton of the Early Permian genus *Labidosaurus*
774 (Reptilia, Captorhinomorpha, Captorhinidae) and the hind limb musculature of
775 captorhinid reptiles. Journal of Vertebrate Paleontology, 9(3):295–313.

776 SUTTON, M. D. 2008. Tomographic techniques for the study of exceptionally preserved
777 fossils. Proceedings of the Royal Society of London B: Biological Sciences,
778 275(1643):1587–1593.

779 SUTTON, M., I. RAHMAN, and R. GARWOOD. 2014. Techniques for Virtual
780 Palaeontology. John Wiley & Sons, Oxford, 208 p.

781 SUTTON, M. D., D. E. G. BRIGGS, D. J. SIVETER, and D. J. SIVETER. 2005. Silurian
782 brachiopods with soft-tissue preservation. Nature, 436(7053):1013–1015.

783 SUTTON, M. D., R. J. GARWOOD, D. J. SIVETER, and D. J. SIVETER. 2012. SPIERS
784 and VAXML; A software toolkit for tomographic visualisation and a format for
785 virtual specimen interchange. *Palaeontologia Electronica*, 15(2):1–14.

786 TAHARA, R., and H. C. LARSSON. 2011. Cranial pneumatic anatomy of *Ornithomimus*
787 *edmontonicus* (Ornithomimidae: Theropoda). *Journal of Vertebrate Paleontology*,
788 31(1):127–143.

789 TRINAJSTIC, K., C. MARSHALL, J. LONG, and K. BIFIELD. 2007. Exceptional
790 preservation of nerve and muscle tissues in Late Devonian placoderm fish and their
791 evolutionary implications. *Biology Letters*, 3(2):197–200.

792 VINTHER, J. 2015. A guide to the field of palaeo colour. *BioEssays*, 37(6):643–656.

793 VON BACZKO, M. B., and J. B. DESOJO. 2016. Cranial anatomy and palaeoneurology of
794 the archosaur *Riojasuchus tenuisiceps* from the Los Colorados Formation, La Rioja,
795 Argentina. *PloS one*, 11(2):e0148575.

796 WALSH, S. A., P. M. BARRETT, A. C. MILNER, G. MANLEY, and L. M. WITMER.
797 2009. Inner ear anatomy is a proxy for deducing auditory capability and behaviour in
798 reptiles and birds. *Proceedings of the Royal Society of London B: Biological*
799 *Sciences*, 276(1660):1355–1360.

800 WALSH, S. A., A. N. IWANIUK, M. A. KNOLL, E. BOURDON, P. M. BARRETT, A. C.
801 MILNER, R. L. NUDDS, R. L. ABEL, and P. D. STERPAIO. 2013a. Avian
802 cerebellar floccular fossa size is not a proxy for flying ability in birds. *PloS one*,
803 8(6):e67176.

804 WALSH, S. A., Z.-X. LUO, and P. M. BARRETT. 2013b. Modern imaging techniques as a
805 window to prehistoric auditory worlds, p. 227–261, *Insights from Comparative*
806 *Hearing Research*. Springer.

807 WILBY, P. R., and D. E. G. BRIGGS. 1997. Taxonomic trends in the resolution of detail
808 preserved in fossil phosphatized soft tissues. *Geobios*, 30:493–502.

809 WITMER, L. M. 1995. The extant phylogenetic bracket and the importance of reconstructing
810 soft tissues in fossils, p. 19–33. *In* J. J. THOMASON (ed.), *Functional morphology in*
811 *vertebrate paleontology*. Cambridge University Press.

812 WITMER, L. M. 1997. The Evolution of the Antorbital Cavity of Archosaurs: A Study in
813 Soft-Tissue Reconstruction in the Fossil Record with an Analysis of the Function of
814 Pneumaticity. *Journal of Vertebrate Paleontology*, 17(sup001):1–76.

815 WITMER, L. M. 2001. Nostril position in dinosaurs and other vertebrates and its significance
816 for nasal function. *Science*, 293(5531):850–853.

817 WITMER, L. M., S. CHATTERJEE, J. FRANZOSA, and T. ROWE. 2003. Neuroanatomy of
818 flying reptiles and implications for flight, posture and behaviour. *Nature*,
819 425(6961):950–953.

820 WITMER, L. M., and R. C. RIDGELY. 2008. The paranasal air sinuses of predatory and
821 armored dinosaurs (Archosauria: Theropoda and Ankylosauria) and their contribution
822 to cephalic structure. *The Anatomical Record*, 291(11):1362–1388.

823 WITMER, L. M., and R. C. RIDGELY. 2009. New insights into the brain, braincase, and ear
824 region of tyrannosaurs (Dinosauria, Theropoda), with implications for sensory
825 organization and behavior. *The Anatomical Record*, 292(9):1266–1296.

826 WITMER, L. M., R. C. RIDGELY, D. L. DUFEAU, and M. C. SEMONES. 2008. Using CT
827 to peer into the past: 3D visualization of the brain and ear regions of birds, crocodiles,
828 and nonavian dinosaurs, p. 67–87, *Anatomical imaging*. Springer.

829 WROE, S., U. CHAMOLI, W. C. H. PARR, P. CLAUSEN, R. RIDGELY, and L. WITMER.
830 2013. Comparative biomechanical modeling of metatherian and placental saber-

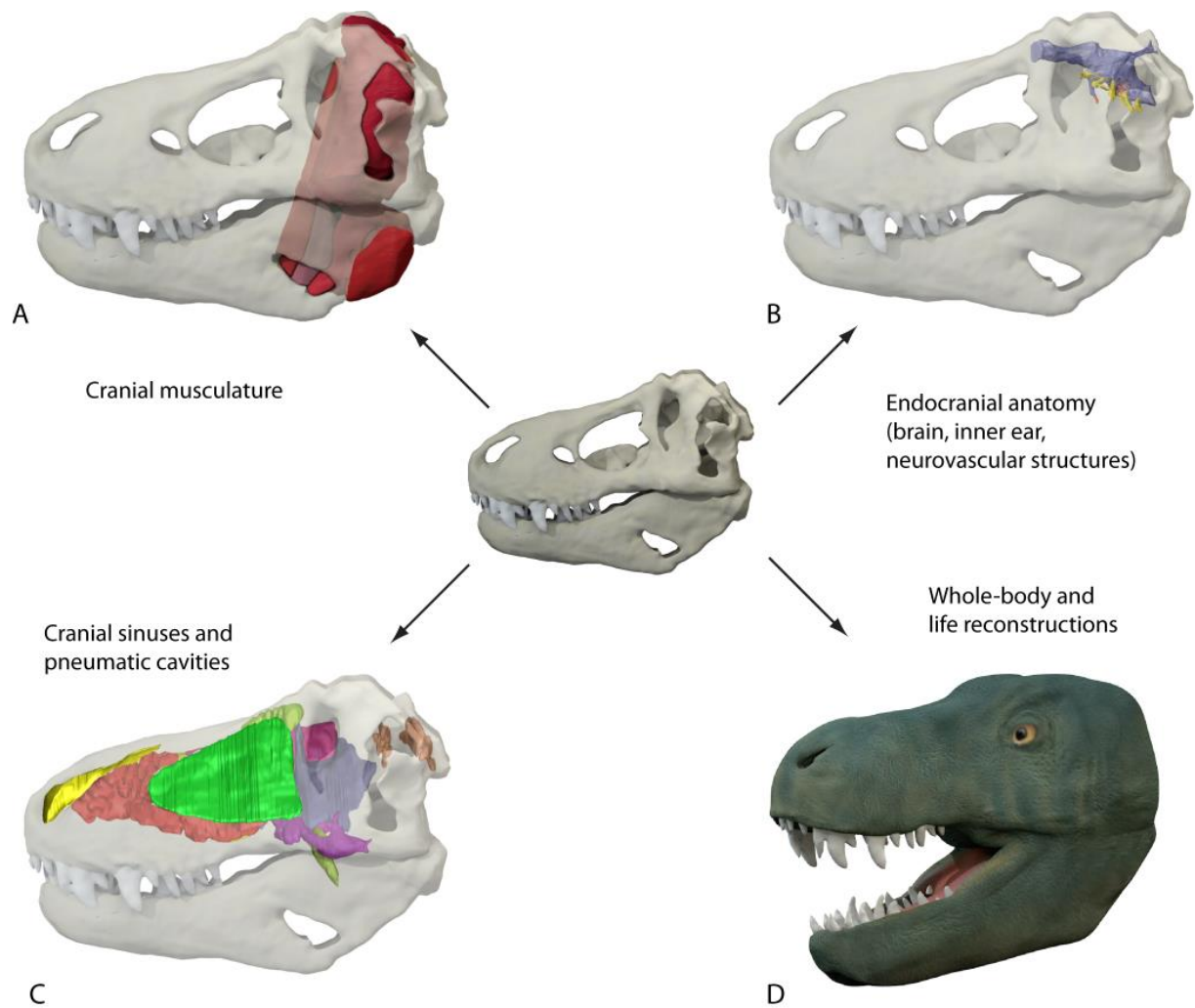
831 tooths: a different kind of bite for an extreme pouched predator. PloS one,
832 8(6):e66888.

833 ZELENITSKY, D. K., F. THERRIEN, R. C. RIDGELY, A. R. MCGEE, and L. M.
834 WITMER. 2011. Evolution of olfaction in non-avian theropod dinosaurs and birds.
835 Proceedings of the Royal Society of London B: Biological Sciences, 278(1725):3625–
836 3634.

837 ZOLLIKOFER, C. P., M. S. P. DE LEÓN, D. E. LIEBERMAN, F. GUY, D. PILBEAM, A.
838 LIKIUS, H. T. MACKAYE, P. VIGNAUD, and M. BRUNET. 2005. Virtual cranial
839 reconstruction of *Sahelanthropus tchadensis*. Nature, 434(7034):755–759.

840 ZOLLIKOFER, C. P. E., M. S. PONCE DE LEÓN, R. W. SCHMITZ, and C. B.
841 STRINGER. 2008. New Insights Into Mid-Late Pleistocene Fossil Hominin Paranasal
842 Sinus Morphology. The Anatomical Record: Advances in Integrative Anatomy and
843 Evolutionary Biology, 291(11):1506–1516.

844



845 C

846 FIGURE 1.—Digital reconstruction of main cranial soft-tissue structures exemplified by

847 *Tyrannosaurus rex*: (A) reconstructed jaw adductor musculature; (B) reconstructed endocranial

848 components (brain, inner ear, and neurovascular structures) modified from Witmer and Ridgely

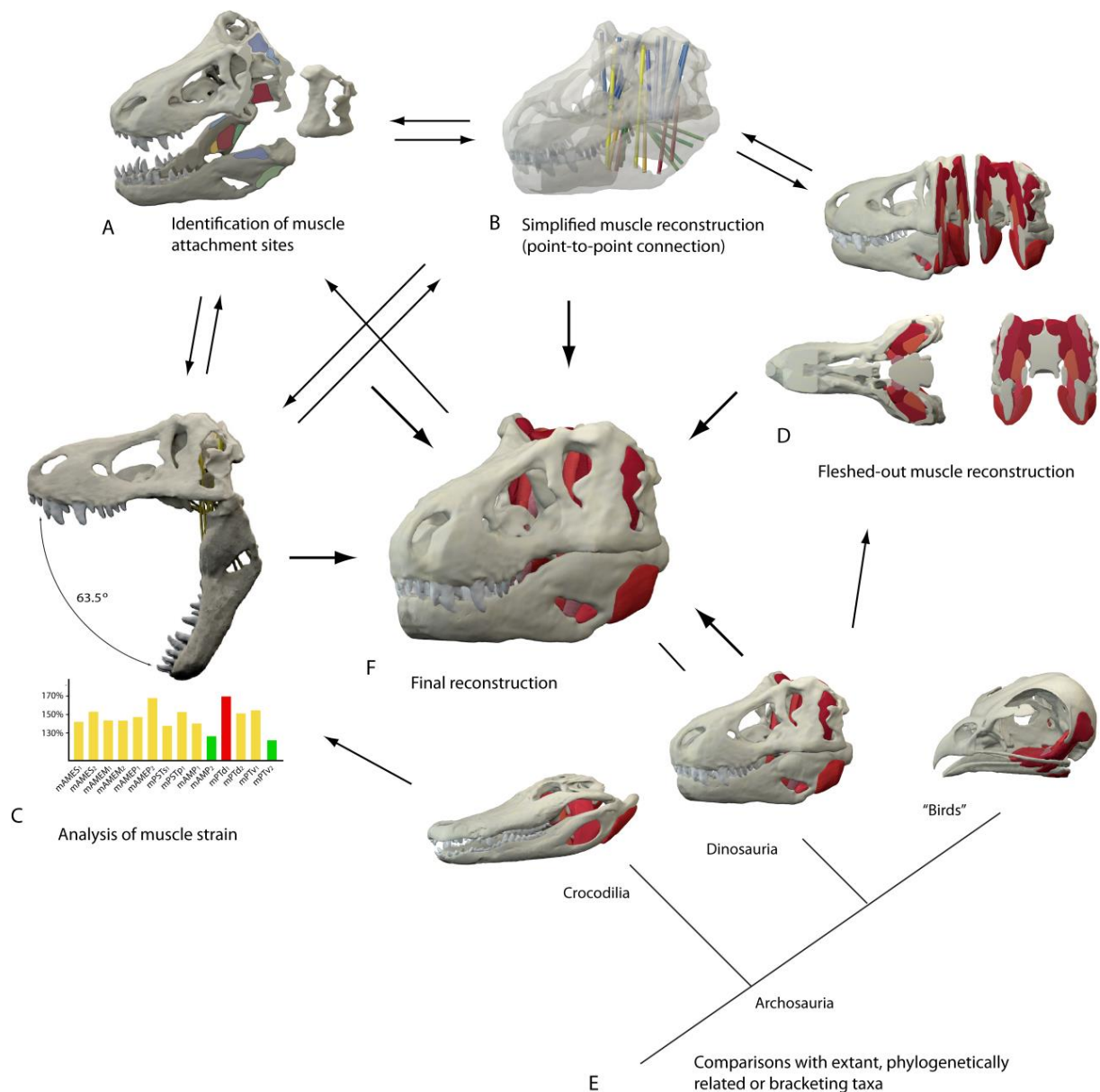
849 (2009); (C) reconstructed paranasal sinuses and associated structures (airway, olfactory, and tympanic

850 regions) modified from Witmer and Ridgely (2008); (D) life reconstruction based on osteological

851 model.

852

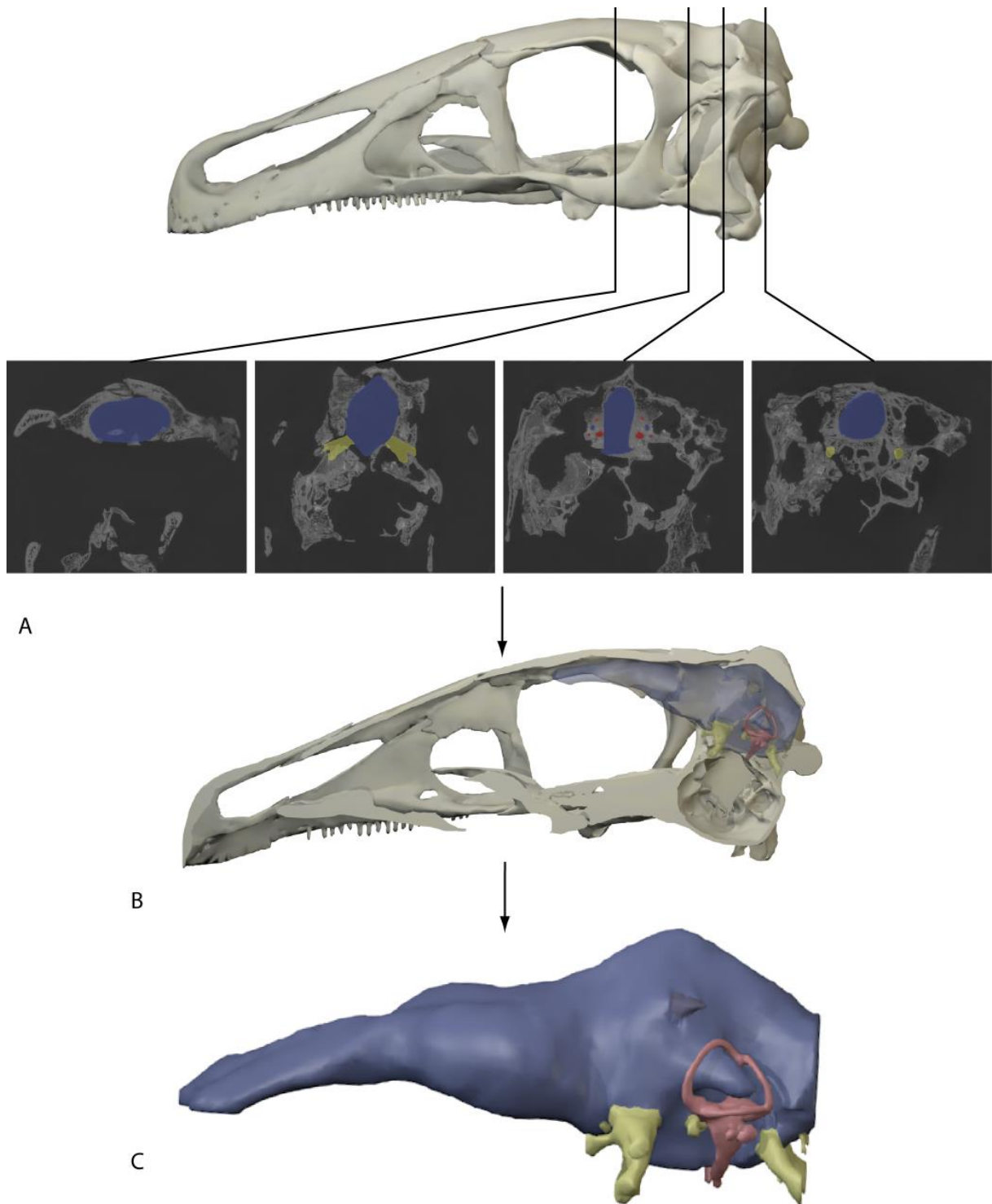
853



854

855 FIGURE 2.—Different procedures applicable to reconstruct the jaw adductor musculature
 856 exemplified by *Tyrannosaurus rex*: (A) identification of muscle origins and insertions based on
 857 osteological correlates; (B) simplified muscle reconstruction (“cylinder model”) using point-to-point
 858 connections between corresponding muscle attachments (based on Lautenschlager, 2013); (C)
 859 analysis of muscle strain capabilities (Lautenschlager, 2015); (D) fleshed-out muscle reconstruction
 860 based on cylinder model and topological constraints (based on Lautenschlager, 2013); (E)
 861 comparisons with extant taxa, which are phylogenetically closely related or form an extant
 862 phylogenetic bracket; (F) final muscle reconstruction.

863



864

865 FIGURE 3.—Digital reconstruction of the endocranial anatomy exemplified by *Erlikosaurus*

866 *andrewsi*: (A) examples of segmented CT slice data of the cranial skeleton of *Erlikosaurus andrewsi*;

867 (B) endocranial components in-situ and rendered transparent; (C) reconstructed endocranial

868 components.